Study the Effect of Wind Speed on the Dynamic Stall Behaviour of Horizontal Axis Wind Turbine Performance Characteristics During Yaw Misalignment using Analytical Approach

E. S. Abdelghany *, Mohamed B. Farghaly **‡

* Mechanical Engineering Department, Faculty of Engineering, Albaha University KSA, on Leave from Institute of Aviation Engineering and Technology, Egypt

** Mechanical Engineering Department, Faculty of Engineering, Fayoum University, 63514, Fayoum, Egypt

(Eslam_said312002@yahoo.com, eslam@bue.edu.sa ; mbs12@fayoum.edu.eg , bader_pilot@yahoo.com)

‡Corresponding Author; Mohamed B. Farghaly, Mechanical Engineering Department, Faculty of Engineering, Fayoum University, keman Faras Street, Fayoum 63514, Egypt, Tel: +20 100 820 0258, mbs12@fayoum.edu.eg, bader_pilot@yahoo.com

Received: 08.02.2023 Accepted: 17.04.2023

Abstract- The stall phenomena are essentially important in the design and operation of the several aerodynamic applications especially for rotating wings such as wind turbines. This phenomenon is considered the primary cause of the unsteady loads on blades profile and has a negatively impacts in the aerodynamic characteristics, turbine fatigue life, and the accurate prediction of these loads are becomes essential. This process contributes to an increase in the aerodynamic loads over the blade profile when the turbine blade sectional attack angles are rapidly exceeds the static stall attack angle because gusts, turbulence in-flow, and yaw-misalignment. This research aims to study the effect of wind speed on the behaviour of dynamic stall of horizontal axis wind turbine performance characteristics in the presence of yaw-misalignment. The blade profile was modelled using S809 airfoil. The mathematical model was created and adopted using MATLAB software based on the blade element momentum theory. The Beddoes–Leishman model in the existence of yaw-misalignment was tailored and implemented in the created code for wind turbine applications. The variations of turbine performance characteristics with the rotor azimuthal angles and flow attack angle were predicted and discussed for various wind speeds at several span-wise sections along the rotor blade length and the appropriate flow control techniques at critical areas were suggested. The obtained results illustrate that the phenomena of the dynamic stall occur mainly at the inboard stations of rotor blade, and the hysteresis values of the normal force coefficient loops is greater than the tangential force coefficient loops.

Keywords Wind Turbine Performance, Dynamic Stall Phenomena, Reduced Frequency, Yaw Misalignment, Leishman–Beddoes Model.

NOMENCLATURE

Symbol	Meaning and units	Symbol	Meaning and units
HAWT	Horizontal Axis Wind Turbine	λ	Tip speed ratio
CFD	computational fluid dynamic	θ_P	Blade pitch angle (Degree)
NREL	National Renewable Energy Laboratory	r	Radius of the considered section
DS	Dynamic stall	θ_{tw}	Local Twist angle (Degree)
TE	Trailing edge	U_R	Wind speed at the rotor plane
L.E	Leading edge	U_0	Unperturbed wind speed
CFJ	Co-flow jet	Ψ	Blade azimuth angle
BEM	Blade element momentum	β	Yaw angle

TEF	Trailing edge flaps	α	Attack Angle (Degree)
TWL	Tip Winglet	c	Airfoil chord length
MRT-LBM	Multi-relaxation time lattice Boltzmann	C_n	Normal force coefficients
NVLM	Nonlinear vortex latticemethod	C_t	Tangential force coefficients
VPM	Time-accurate vortex particle method	k	Reduced frequency
VGs	vane-type vortex generators	θ	Pitch angle
U_{wind}	Wind speed vector	σ	Local solidity
Ω	Blade's angular velocity	M	Mach numbers
V_{eff}	Local effective velocity	Cn;I	Critical coefficient of normal force
a	Axial induction factor	ω	Excitation frequency
a´	Tangential induction factor	Φ	Inflow angle

1. Introduction

Several wind turbine farms operate most of time in stations of adverse, unsteady, and turbulent environments. This environment may cause changes in the loads applied along the rotor blade span especially because of the turbine yawing according to the direction of blowing wind. Also, the yawning of wind turbine rotor leads to a large fluctuation in the velocity of relative flow at the leading edge (LE) of turbine blade profiles. In wind turbine blades, the problems associated with the unsteadiness flow are serious which can lead to some critical problems such as the dynamic stall (DS) phenomena. This phenomenon is considered one of the significant unsteady aerodynamic problems taking place on most rotary wings such as the aircraft propeller blades, helicopter main rotor blades, and the turbine blades. Understanding the aerodynamics behaviour around the turbine blades in different operating conditions is considered one of the most significant key factors to predict and improve their characteristics [1]. The basic physical features and the main attempts which have been done to guess the phenomenon of the dynamic stall were summarized, most information presented have come from much experimental research, the details of dynamic stall parameters are analysed principally in some physical terms [2, 3]. The Laboratory data set of the National Renewable Energy "Combined Experiment" was analysed to deliver a mathematical assessment of the dynamic stall frequency occurrence over a HAWT during the typical operating conditions, according to the obtained results it was found that, the dynamic stall for yawed HAWT was seen to appear for about more than 50% of the recorded cycles, also the dynamic stall occurrence at all station but at the 30% of blade span (inboard station) shows a good agreement compared with the theoretical limits [4]. The complex flow characteristics during the dynamic stall development over the wind turbine rotor blades were investigated experimentally using a scaled 3-D turbine blade model, the measured data show that the transition from the attached airflow to the complete stall was delayed to a higher attack angle and appears at the higher rate compared with transition from the complete stall to the attached airflow [5]. Recently, computational fluid dynamics techniques have shown success for modelling dynamic stalls in wind turbine applications and have become increasingly practical with increasing computational power [6]. The numerical model of detached-eddy simulation coupled with the computational fluid dynamics techniques was used to investigate the dynamic stall behaviours around turbine blade profile of the NREL (Phase-VI), the results computed of blade characteristics were compared to some experimental data of unsteady experiment, the obtained computational results indicate that the distributions of pressure and the coefficients of force fairly well [7]. Recently, the analysis of DS around airfoil section of S809 was performed numerically in combining with the modified model of Leishman–Beddoes that used for DS of the applications of wind turbine. Coefficients of moment, drag, and lift were compared to the experimental data of the oscillating S809 for several reduced frequencies, attacked angle, and the obtained results of modified model indicate a respectable agreement with experimental data [8]. The DS control of the S809 airfoil section is examined computationally using the Co-Flow Jet (CFJ) implementation, the dynamic stall characteristics were investigated with three different coefficients of jet momentum compared with baseline, the obtained results of this analysis indicates that the extreme of fluctuating of the aerodynamic loads were significantly alleviated and according to the energy analysis, the (CFJ) concept is economical and applicable in controlling the dynamic stall problems [9]. Several studies and researches MPPT methods and hybrid systems and of renewable energy resources are review and explained [10]. The modelling of wind turbine power curve was studied to monitoring turbine operation characteristics and behaviour [11]. The several conversion systems research of the resources of wind energy in a smart grid are review and described [12]. Improving the aerodynamic performance characteristics and maximize the turbine efficiency using trailing-edge flap as a flow control device was computationally investigated for various wind speed ranges and several flap deflections [13]. The dynamic stall behaviour of horizontal axis wind turbine in the presence of yaw-misalignment were studied for constant flow conditions, the effect of dynamic stall phenomenon on the turbine performance characteristics were investigated, the obtained results illustrate that the dynamic stall phenomena are occur mostly at the inboard sections, and no longer be influenced by the number of revolution (N) [14]. The experimental and numerical analysis in yawing behaviour was studied on a small three-bladed HAWT prototype, the behaviour of turbine performances (power, thrust coefficients) is predicted as a function of the azimuth angle, the obtained results show that, the intensity of fluctuation decreases with the yaw angle [15]. The cyclic load of the wind turbine load fluctuation was studied experimentally at different tip-speed ratios and several yaw angles, the variation of turbine performance characteristics with the rotor azimuth position were predicted and compared with the NREL FAST code predictions under the same

operation conditions [16]. The aerodynamic performance characteristics of the specific wind turbine rotor and the dynamic changes in the near-wake under a process of sine yawing were investigated using the multi-relaxation time lattice Boltzmann (MRT-LBM) model, the obtained results indicate that, for the condition of dynamic yaw, the degree of stability of the tip spiral wake is inversely related to the absolute value of the change rate of yaw angular speed [17]. The skewed wake effects on the unsteady aerodynamic behaviour of wind turbine rotor blade under yawed flow conditions were investigated numerically using the coupling between the nonlinear vortex lattice (NVLM) and time-accurate vortex particle (VPM) methods [18]. The effect of the vane-type vortex generators on the dynamic stall behaviours of a NREL S809 airfoil section equipped with VGs were investigated, the URANS simulations are used to identify the characteristics of the unsteady flow, the effect of VGs height and chordwise on the unsteady aerodynamics characteristics undergoing dynamic stall were predicted [19]. Generally, the airfoil section of any rotary wings experiences the dynamics stall phenomenon when two main conditions are met: higher values of the flow attack angle (larger than the static stall value), and large enough reduced frequency. If these conditions are satisfied, the dynamics stall phenomenon imposes large load amplitude on airfoil section for same range of attack angle compared to the characteristic of airfoil in the case of static loading. In the case of wind turbine blades, the DS can be occurred because of several parameters such as unsteady inflow, turbulence flow, off-axis operation, tower shadow, wind shear, yaw misalignment, and finally rapid increases in the speeds of wind or gusts, all these parameters are contributed to the high changes in the attack angle at each section along the blade length. As a result, the blades of turbine rotors can experience face drag and lift forces that are usually greater than would be expected in the case of static operation alone. This increases in the aerodynamic forces will have several negative effects especially on the performance change and increasing the bending loads of the turbine rotor. Since the rotor blades of the wind turbine are facing a high increase in the lift forces, the loads of gust are more dangerous than the loads of stall and sometimes, able to break the blades of turbine [20]. The subsequent effect of the deep stall can lead to an increase in the blade vibrations, which lead to some adverse effects on the turbine lift and therefore boost the costs of maintenance associated with turbine operation. This study aims to investigate the wind speed effect on the behaviour of dynamic stall of horizontal axis wind turbine (HAWT) performance characteristics in the existence of yaw-misalignment using analytical approach. The turbine blade profile was modelled using S809 airfoil section. The mathematical model was created and adopted using MATLAB software based on theory of Blade-Element-Momentum (BEM). The classical dynamic stall model of Beddoes–Leishman was used to predict the load variation due to the stall phenomenon by implement them in conjugated with the BEM generated code. The variations of the basic rotor blade parameters with the turbine blade span-wise radius (r/R) were predicted at different operation wind speeds. The variation of the turbine performance characteristics with the rotor azimuthal angles and flow attack angle were investigated and discussed for several span-wise sections along rotor blade length. The variations of axial (a), angular (a') induction factors, tangential and normal (C_t, C_n) coefficients of force were investigated at different stations along the turbine blade length for various operating wind speeds. Finally, the effect of stall behaviours on the turbine characteristics were evaluated, the regions along the turbine blade span which required dynamic stall control are determined, and the appropriate flow control techniques are suggested according to dynamic stall behaviours at each region along the blade span.

In later studies, most researchers are concentrated mainly on the investigate the dynamic stall behaviours using computational and experimental measurements, while the novelty of the current study centric on modelling the dynamic stall problems in the wind turbine applications in a simplified form using analytical approaches by generate a general codes based on the BEM theory in conjugate with the appropriate dynamic stall model using in the case of rotary wings such as the classical Beddoes–Leishman dynamic stall model.

2. Dynamic Stall Phenomena

2.1. Physical Descriptions

The dynamic stall is considered one of main sources of loads fluctuation applied on the turbine blades. This phenomena leads to stall delay and then extreme increase in the generated lift force especially when the static stall angle is rapidly exceeded [21]. This phenomena occurs when the airfoil is subjected to an oscillation in the flow attack angle beyond the value of static stall conditions. This means a subsequent various phenomena took place, with a complicated in the general behaviour in the loads around airfoil, which will produced a very different in the aerodynamic forces than those obtained during static operation conditions [22].

2.2. Dynamic Stall - Five Stages

To better understand this complicated phenomenon, the flow behaviour was divided into five stages, as explained in the Fig.1. In stage-I, the value of attack angle is increased rapidly that is leads to reduction in the gradients of adverse pressure along airfoil chord compared with the same attack angle in case of quasi-steady flow, this will leads to delay the start of flow separation as illustrate in Fig.1a. In stage-II, the values of attack angle are further augmented, the point of flow separation approaches adjacent to the airfoil leading-edge (LE), and the vortices with intermediate strength has generated at this region as illustrated in Fig.1b. At this stage the vortex disturbance will be initiated from airfoil (LE) and moved toward the down-stream through the airfoil chord which will cause movement the centre of pressure at the aft direction and subsequently a great nose-down pitching moment will occur, generally this stage called as the moment stall. If this disturbance of vortex stays above the airfoil upper surface, it will lead to deliver additional lift. Stage-III, this stage was characterized by a rapid breakdown in the coefficient of lift, which occurs at attack angle higher than

the attack angle of the sudden decrease in the pitching moment, which means that, the moment of stall will happen at the beginning of the vortex shedding, but the stall of lift will occur just when the vortex shedding passes through the wake formations. In this stage the upper surface airflow becomes completely separated as presented in Fig.1c. Stage-IV, this stage is designated when the disturbance of the vortex shedding passes through the airfoil trailing-edge (TE), the lift stall and airflow progresses to the full separation as illustrated in Fig.1d. Stage-V, this stage is designated when the flow reattachment front to back is significantly lagged as illustrated in Fig.1e. In this stage the full reattachment of the airflow is delayed to configurations at stall angle lower than the angle of stall in normal static case.

(a) (b) (c) (d) (e)

Fig. 1. Stages of dynamic stall, (a) Stage-I, (b) Stage-II, (c) Stage-III, (d) Stage-IV, (e) Stage-V.

2.3. Modelling

The dynamic stall behaviours include a set of complex phenomena as explained and discussed above, and the attempting to generate a mathematical model to predict its effects not simple. Aerodynamicists, specifically persons have involved in the analysis and design of helicopter rotors have been working on the dynamic stall assignment since 1960's. Presently the most models that attempt to predict the effect of dynamic stall are simple semi-empirical or empirical models and it have a behaviour mostly like the CFD approaches. The appropriate computational simulation can be achieved by resolving the complete Navier-Stokes-Equations coupled with an appropriate model of turbulence to approach the nature stall phenomena that are presented in the realistic dynamic stall [23, 24].In general, a two types of stall models that are used to investigate the effect of dynamic stalls, one of them is so-called the "Engineering Models" and the others is "Semi-Empirical Models". The engineering models' techniques are based on resynthesizing the measured aerodynamic loads on unsteady airfoil to try to recreate the perceived experimental trends. In contrast, the models of semi-empirical techniques are based on descripe the simplified simulations of the dynamic stall physical means by using a set of linear and non-linear mathematical equations to represent the loads in cases of un-steady airfoil. These models always required many empirical parameters which are usually obtained from the unsteady and steady experiments for several developed airfoils shapes at different operation conditions. The Leishman-Beddoes method is considered one of the important methods which used to assess the unsteady drag force, lift force, moment, and it characterized by having an additional complete depiction of the physical problem of un-steady aerodynamic loads prediction which extensively confirmed with several data of experiment. This approach assumes the process of DS is begins when the equivalent parameter of pressure at (LE) of airfoil reaches the critical values. This approach yields moderately good predictions of unsteady aerodynamic loads, also it has a significant advantage which it needs little empirical coefficients which are find from the data of airfoil in the static condition, and this clarifies why this model is so common and has been widely utilized in the prediction loads of helicopter rotor. The results of this model are compared with an experimental database of unsteady measurements of some airfoils to validate it [25, 26, 27].

2.4. The concept of reduced frequency

As previously mentioned, when the flow attack angle rapidly changes, the aerodynamic loading on the blade profiles were affected simultaneously due to the dynamic stall behaviours. Also, the airfoil response to the local flow changes is not only dependent upon the excited frequency (ω) but it related to many parameters such as the airfoil chord (c), airflow local velocity (U), especially when the perturbation speed of propagation is limited, and the response of airfoil undergoing fluctuations are described by reduced the frequency (k), which will be described as shown in Eq. (1):

$$k = (\omega * c) / 2U \quad (1)$$

According to the Leishman- model, we can consider that:

- If ($k < 0.05$), the problem is considered as quasi-steady and the effect of unsteady flow is usually slight and can be ignored (i.e.,quasi-steady problem)
- If ($k > 0.05$), the problem is considered as unsteady, and thus to perform an accurate analysis, the terms of unsteady in equations cannot be neglected.
- If ($k > 0.2$), the problem is considered as highly unsteady, and the unsteady terms in equations will dominate the behavior of the aerodynamic loads.

3. Aerodynamics Design of Horizontal Wind Turbine

The main objective of this section is study and discuss the general aerodynamic characteristics of the horizontal axis wind turbine sections and illustrate the effect of stall delay (rotational augmentation) on the behaviours of lift and drag coefficients at the different blade stations along the blade span. Finally, take these effects into consideration when generated the dynamic stall simulation code using the commercial software like MATLAB programming.

3.1. Airfoil Aerodynamics

To understand and analyses the flow characteristic on any rotating blade, the theory of blade element momentum (BEM) has been used. Fig.2 illustrate the main convention parameters of local airfoil section along the turbine rotor blade [28, 29]. Where: U represent the incoming speed of

wind, Ω is the rotor angular velocity, V_{eff} represent the effective velocity around airfoil, (a´, a) are the tangential and axial induction factors, Φ is the inflow angle, θ the total angle of pitch, α is the attack angle, and r represent the radius at considered sectional on the blade. From Fig.2 we can note that the effective velocity of the considered sectional airfoil has two components, one of them in the direction of turbine rotor plane and the other orthogonal to the turbine rotor plane. These velocity components are affected by tangential and axial (a', a) induction factors respectively. In general, these induction factors are presented to compensate the effect of rotating blades on the air stream before reached to the plane of turbine rotor, and automatically the effective airflow velocity at the turbine plane of rotor is significantly changed from normal flow unperturbed condition.

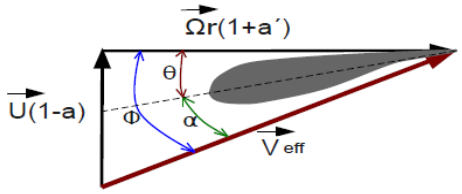

Fig. 2. Rotating Blade Airfoil Section Convention [28].

From Fig.2, it is shown that, keeping constant angular velocity, the increase in the speed of wind will increase attack angle of airfoil at working sections, since the incidence is proportionate to the wind speed to angular velocity ratio. According to some geometric issues, the angle of attack is determined by using Eq. (2), also the total angle of pitch is a combination between both blade pitch angle (θ_P) and local twist (θ_{tw}) and can be determined by using Eq. (3).

$$\alpha = \Phi - \theta = \tan^{-1}[U(1-a)/\Omega r(1-a')] - \theta \quad (2)$$

$$\theta = \theta_P + \theta_{tw} \quad (3)$$

3.2. Aerodynamic Radial Dependency of Sectional Coefficients

In the rotary wings, the stall delay effect at the inboard stations of blade is generally named (rotational augmentation). Near the turbine blade root, the spanwise stations usually work at high attack angles and will experience high amplitude when the yaw-misalignments of turbine rotor exist. Then to evaluate the DS model characteristics, mainly at the inboard stations of turbine rotor, it is thus important to involve the stall delay effect on the coefficients of aerodynamic along the blade sections. The improvement equation of Snel. [29] was used to investigate the coefficient of lift and then implemented in the DS model, as shown in Eq. (4):

$$C_{l,3D} = C_{l,2D}{}^{3}\,(c/r)^2\,\Delta C_l \quad (4)$$

Where, c/r is the percentage of local section chord to radius, ΔC_l is the difference between the potential and static coefficient of lift at different turbine section. The improvement equation of Chaviaropoulos, Hansen [30] was used to investigate the coefficient of drag and then implemented into the DS model, as shown in Eq. (5):

$$C_{d,3D} = C_{d,2D} + 2.2\,(c/r)\cos^4(\theta_{tw})\,\Delta C_d \quad (5)$$

Where, θ_{tw} represent the local angle of twist at blade station and ΔC_d is the difference between 2-D coefficient of drag and coefficient of drag found at zero attack angle. According to the concept of Chaviaropoulos, Hansen [31] and Pereira [26], the correction equations of both drag and lift coefficients were useful up to an attack angle of about 25°, after which the improvement itself was reduced-linearly to zero at attack angle of about 60°. Also, both improvements equations were applied only from blade root of turbine rotor up to blade span-wise of about 50% (r/R = 0:0.5).

4. Adapting and Implementing the Model of DS in the BEM Generation Code

In this section, the effect of dynamic stall phenomena on the turbine performance characteristics was predicted using appropriate dynamic stall model. The selected dynamic stall model was adapted to suitable the environment of the turbine applications and then implemented into the generated BEM code. In this work, the model of Beddoes–Leishman was selected and adapted to the horizontal wind turbine applications and then implemented into the generated BEM code.

4.1. Beddoes–Leishman Dynamic Stall Model

4.1.1. Model Simplifications and Separation Point Estimation

The Beddoes–Leishman model was originally generated and developed for the applications of aircraft helicopter blades, and consequentially, the compressibility effects the air flow are included. In the environment of the HAWT, the operation Mach numbers are about (M < 0:3); thus, the model of DS was simplified in the current study by assuming the airflow behavior is incompressible. An additional difference between the wind turbine and helicopter blades is the type of used airfoil sections. Usually, the airfoil with thick shapes is used for wind turbine applications, with thicknesses to chord greater than 15%, but the helicopter blades shape is equipped generally with the airfoil sections have a thin profile. According to the DS modeling by Beddoes and Leishman, the greatest critical aspect is to investigate the occurrence separation at the blade (LE). In the novel model, the separation at (LE) is mainly assumed to occur when the critical coefficient of the normal force ($C_{n;l}$) is reached. These values can be found from static airfoil characteristic with taking the coefficient of the normal forces at which a breakdown in pitching moment curves is visible. But, when the thick airfoil sections are used, generally the significant (TE) separation occurs before the (LE) separation. Thus, the coefficient of normal force can be reduced with growing the attack angle before the breakdown in the pitching moment curves arises. This means, the obtained critical coefficient of the normal force (C_n) using the Beddoes and Leishman criteria may correspond to values less than the maximum value of (C_n), which is impractical. Also, in the static characteristics data of the thick airfoils, it can be happened that the break is not clear observable in the curve of angle of attack versus pitching moment versus.

4.1.2. Model Sub-Systems

The original DS model of Beddoes–Leishman is a semi-empirical model composed from three sub-systems according to the aerodynamic loads and flow behaviours as follow [28]:

- Attached airflow model: which is used for the unsteady linear aerodynamic load, where the loads are obtained throughout indicial functions considered the compressibility.
- Separated airflow model: which used for the non-linear aerodynamic load, where the loads are calculated according to theory of Kirchhoff/Helmholtz and the attack angle history that used to reconstruct the non-linear loads based on the quasi-static or static condition of the dynamic equivalent point of separation, and
- DS models: which are used for aerodynamic loads induced by (LE) vortex, these loads are calculated by considering the dynamic properties of the intense (LE) vortexes passing through the airfoil upper surfaces and being converted throughout the down-stream.

4.2. Generated BME Code and DS Model implementation

From the previous discussion, it is recommended that the additional criteria were required to compute the critical coefficient of the normal force accurately for the wind turbine airfoil sections. In the past, several distinct approaches have been derived to simulate and model the aerodynamics characteristics of the HAWT blades. The (BEM) theory is considered one of the simplified methods which have been derivative for several decades; however, it is still used in the present day not only in initial stages of the HAWT design. So, having these factors in mind, the DS model of Beddoes–Leishman was selected to be implemented in the generated BEM code [31, 32]. The (BEM) theory states that, for rotary wings, the momentum variation of the airflow particles through a cylinder covering the turbine rotor disc is equivalent to the forces acting on the rotor blades due to the aerodynamic effect. In the HAWT, the blades of rotor will act to reduce the arriving speed of wind, and it is mutual to express the variation in flow velocity with means of the axial-induction factors (a) or induced velocities as show in Eq. (6):

$$U_R = U_o (1- a) \quad (6)$$

Where, U_R defined the speed of wind at the plane of turbine rotor, U_o defined the unperturbed speed of wind, and (a) is the axial induction factors which are usually calculated iteratively. In spite of there are induced-tangential factors, the (BEM) models do not take them into consideration due to the small magnitudes compared to the axially induced factors.

5. Case Study

In this study, the aerodynamic profiles of the turbine blades airfoil are comprised from S809 with different relative thickness distributions of t/c = [0.25; 0.21; 0.18] in root sections, at mid-span region and nearing the tip of the blade respectively. The S809 airfoil was designed especially for the wind turbine applications used by National Renewable Energy Laboratory (NREL). From previous sections, it was clear that the DS model needs static aerodynamic characteristics of force coefficient in terms of the attack angle as input parameters; in other meaning, both $C_l(\alpha)$, $C_d(\alpha)$ curves for steady condition must be provided to the DS model to investigate the aerodynamic load in the unsteady condition. Also, the behaviour of both the static and dynamic characteristics of the aerodynamic coefficients in terms of the attack angle (both $C_l(\alpha)$ and $C_d(\alpha)$) were needed to know. The comparison data of smooth airfoil profile at a Reynolds number (R_e) of about 10^6, for reduced frequencies approximately between 0.02 and 0.1 were used. According to the selected profiles, the geometry, dynamic and static aerodynamic characteristics in terms of the attack for NREL S809 airfoil section are illustrated in Fig.4 and Fig.5 respectively. Comparison between predicted, measured and hysteresis curves for NREL S809 were done for mean attack angles of 8°, 14°, and 20°, with an 10° oscillation amplitude. For all mean value of attack angle, the comparisons were done for three different reduced frequencies [33, 34]. But the presented data in Fig.5 were selected according to the main specifications of the turbine model in the case study as illustrated in Table 1.

Table 1. Specifications of case study model [14].

Blades number	3	Twist angle at tip	Zero
Rotor speed [rpm]	450	Yaw angle (β) [degree]	20°
Rotor diameter [m]	5	Reduced frequency	0.077
Blade length [m]	2.25	Upstream Velocity [m/s]	5, 8,10

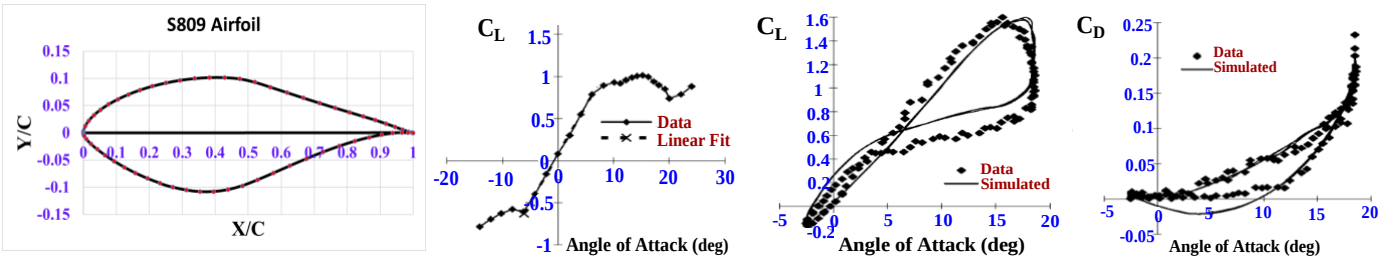

(a) (b) (c) (d)

Fig. 3. NREL S809 airfoil geometry and aerodynamic characteristics, (a) Airfoil geometry, (b) Static lift coefficient versus attack angle, (c) Dynamic coefficient of lift versus attack angle, (d) Dynamic coefficient of drag versus attack angle [27].

6. Methodology

During this work, the blade element momentum (BEM) theory was used to calculate the turbine rotor blade main geometry such as (chord, twist angles, pitch angles, …etc.) distributions according to the turbine design specifications and operation conditions which used in the current study as illustrated in Table 1. The DS model of Beddoes–Leishman was selected, adapted to suitable to the wind turbine applications, and then implemented in conjugate with the generated BEM code. The aerodynamic characteristics versus attack angle for NREL S809 airfoil section in static and dynamic cases (see Fig.3) were inserted as a data base to the generated BEM code. Fig.4 explains the flow chart of how the selected DS model implemented in conjugate with the generated BEM code to compute the aerodynamic coefficients variations at different blade sectional along the blade span.

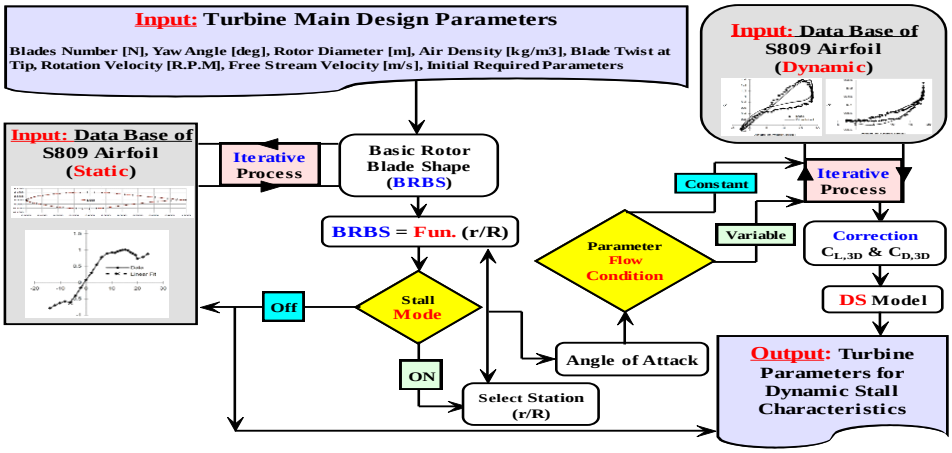

Fig. 4. Complete blade element momentum model diagram coupled with the selected DS model.

7. Result and Discussions

To investigate the effect of DS phenomena on the turbine characteristics, the DS model of Beddoes–Leishman was selected and adapted to suitable the environment of the turbine applications and then implemented in the BEM code of the HAWT. The various operation speed of wind was studied for certain yaw angle (20°) and for constant speed of rotational of about 450 rpm. The wind speed is 5, 8, and 10m/s with tip-speed-ratio (λ) of about 23.6, 14.7 and 11.8 respectively. The variation of the turbine main performance parameters with the azimuthal angles (Ψ) are predicted and discussed for various span-wise sections along the turbine blade span. The tangential and normal force coefficient (C_t, C_n) variation with the attack angle are investigated for various span-wise sections along the turbine blade span. These radial span-wise sections are [r/R = 35%, 50%, and 65%]. In the current study, the turbine rotor was considered rotating in the direction of positive azimuth angle (Ψ), the misalignment of yaw was also in the direction of positive yaw angle ($\beta > 0$).

7.1. Basic Rotor Blade Parameters

The variations of the basic rotor blade parameters with the span-wise of blade length are illustrated in Fig.5, 6, and 7 respectively. Fig.5 illustrates the angular and axial induction (a', a) factors variation with the turbine rotor blade span-wise radius (r/R) at several operation speeds of wind. From Fig.5, it is noted the value of axial induction factor (a) is roughly constant over all blade span-wise, but the angular induction factor (a') is decreased with blade span-wise from root to tip sections. Also, we can note that the angular induction factor (a') is approximately constant at the out portion of the turbine blade especially near blade tip. Fig.6 and Fig.7 illustrate the variation of tangential (C_t) and normal (C_n) coefficients of force with the turbine blade span-wise radius (r/R). From Fig.6, it is noted that the values of normal coefficient of force increases gradually until reaching to the maximum value near the first quarter portion of the turbine blade length and then decrease gradually after r/R=0.4 reaching to the minimum value at the turbine blade tip. From Fig.7, it is noted that the tangential (C_t) force coefficients were decreased gradually with the turbine blade span-wise from root to tip sections and the lowest value appeared near the tip of blade.

7.2. Axial and Angular Induction Factors with Azimuth Angle

The variation of static and dynamic axial induction (a) factors with the rotor azimuth angle (Ψ) for various span-wise sections along the turbine blade span were predicted at different operation wind speed as shown in Fig.8 and 9 respectively. From Fig.8, it is noted that the values of axial induction factor in static case are approximately constant for all blade span-wise along the turbine radius and for all operation wind speed. From Fig.9, generally it is noted that the dynamic axial induction factor values are decreased gradually with an increase in the turbine blade span-wise ratio from the blade root to tip sections. Also, we can note that, the change in the dynamic axial induction factor values appears near the inboard stations of the turbine blade (r/R= 35%) and it have slightly changed at stations of out portion at the turbine blade (r/R= 50% and 65%) and the lowest values appeared near the tip of blade. The variation of static and dynamic angular induction (a') factors with the rotor azimuth angle (Ψ) for various span-wise sections along the turbine blade span were predicted at different operation wind speed

as shown in Fig.10 and Fig.11 respectively. From these figures, it is noted that the static and dynamic angular induction factors have the same behaviours of the axial induction factor values discussed in Fig.8 and 9.

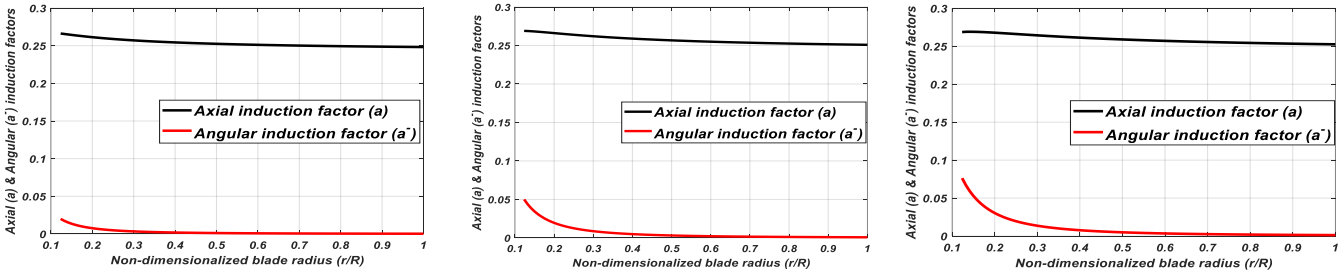

(a) (b) (c)

Fig. 5. Variation of static axial induction factors with span-wise sections at different operation wind speed and 1 revolution, (a) At 5m/s, (b) At 8m/s, (c) At 10m/s.

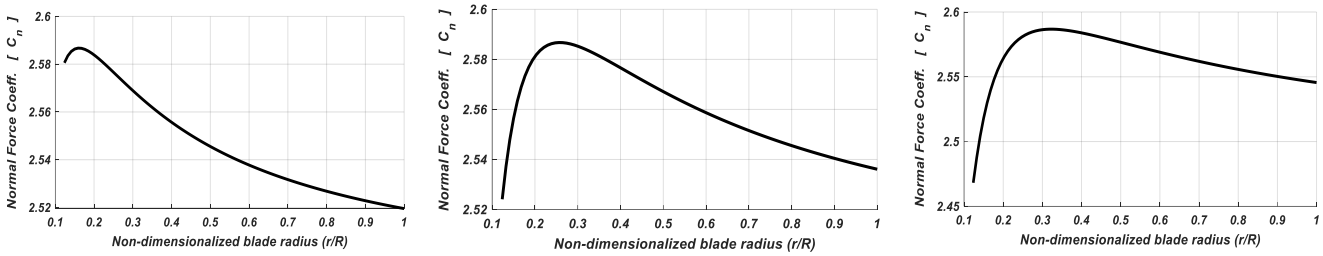

(a) (b) (c)

Fig. 6. Variation of normal force coefficients with span-wise sections at different operation wind speed and 1 revolution, (a) At 5m/s, (b) At 8m/s, (c) At 10m/s.

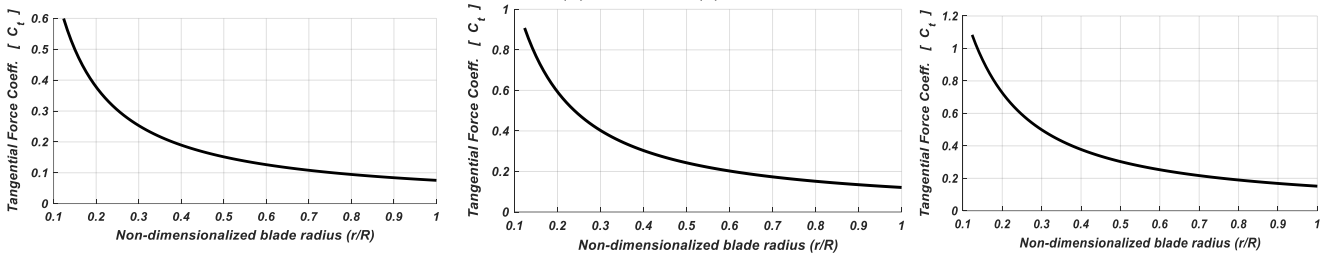

(a) (b) (c)

Fig. 7. Variation of tangential force coefficients with span-wise sections at different operation wind speed and 1 revolution, (a) At 5m/s, (b) At 8m/s, (c) At 10m/s.

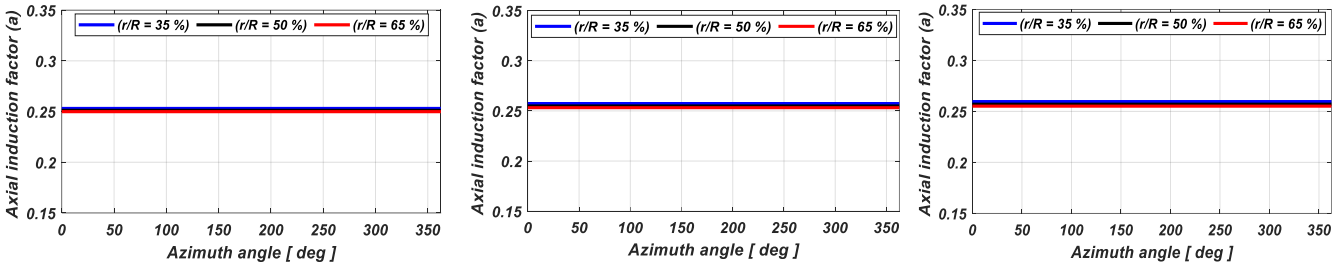

(a) (b) (c)

Fig. 8. Variation of static axial induction factors with azimuth angle for several span-wise sections at different operation wind speed and 1 revolution, (a) At 5m/s, (b) At 8m/s, (c) At 10m/s.

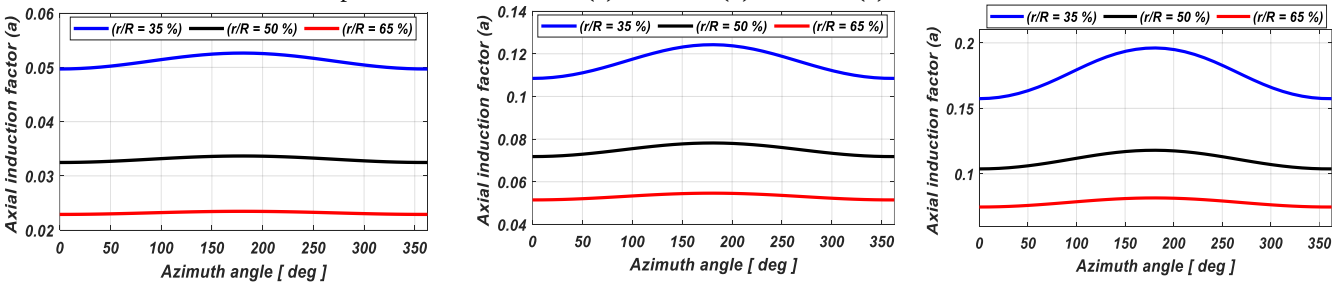

(a) (b) (c)

Fig. 9. Variation of dynamic axial induction factors with azimuth angle for several span-wise sections at different operation wind speed and 1 revolution, (a) At 5m/s, (b) At 8m/s, (c) At 10m/s.

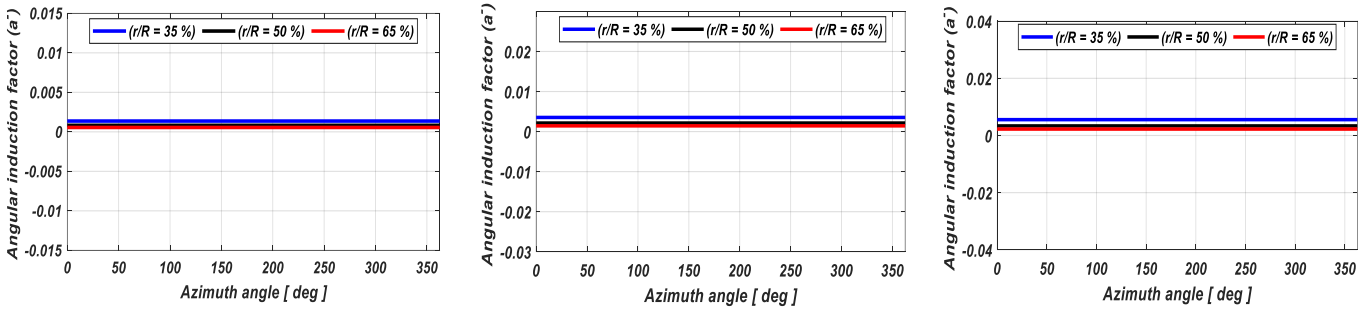

(a) (b) (c)

Fig. 10. Variation of static angular induction factors with azimuth angle for several span-wise sections at different operation wind speed and 1 revolution, (a) At 5m/s, (b) At 8m/s, (c) At 10m/s.

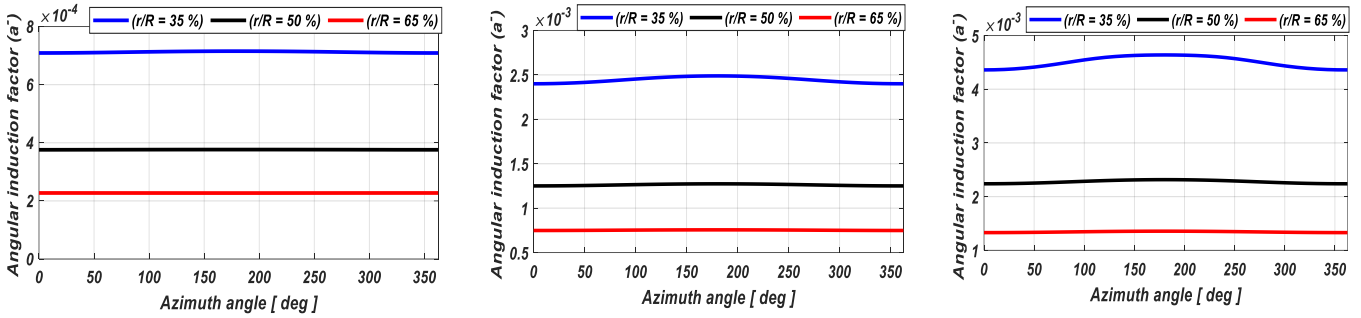

(a) (b) (c)

Fig. 11. Variation of dynamic angular induction factors with azimuth angle for several span-wise sections at different operation wind speed and 1 revolution, (a) At 5m/s, (b) At 8m/s, (c) At 10m/s.

7.3. Tangential and Normal Coefficients of Force with Rotor Azimuth Angle

The variation of normal (C_n) and tangential (C_t) coefficients of force with the rotor azimuth angle (Ψ) for various span-wise sections along the turbine blade span were predicted at different operation wind speed as shown in Fig.12 and Fig.13 respectively. From these figures, it is noted that, the values of the normal and tangential coefficients of force were decreased gradually on the first and second quarter of blade rotation azimuth angle (Ψ = 0 :180 deg.) and then increases gradually on the third and fourth quarter of blade rotation azimuth angle (Ψ = 180 :360 deg.). Generally, it is noted that the average values of tangential and normal force coefficient are decreased with increase the turbine blade span-wise ratio from the turbine root sections to tip sections but increased with increase in the flow wind speed as illustrated in Fig.12 and Fig.13. The peaks of maximum and minimum values are changed according to the span-wise sections along the turbine blade span. From these figures, it can note that, as the speed of wind increases the amplitude of the normal and tangential coefficients of force was increased and, the amplitude of normal force coefficient (C_n) increases as the blade spanwise section is closed to the turbine blade tip but in contrast the amplitude of tangential force (C_t) coefficient is decreases.

7.4. Tangential and Normal Force Coefficients with Attack Angle

To illustrate the effect of stall phenomena on the turbine main parameters, the variation of tangential and normal (C_t, C_n) coefficients of force with attack angle (α) was predicted and plotted for several operation wind speed at different spanwise along of blade length of (r/R=35%, 50%, and 65%) as shown in following figures. Fig.14 illustrates the normal coefficient of force variation with the attack angle (C_n-α) at different spanwise along of blade length for operating wind speed range of 5m/s, 8m/s, and 10m/s respectively. From these figures, generally it is show that, the values of the normal force coefficient were increased until reaching to the maximum value and then decrease gradually until reaching to the minimum values and after reach to the minimum value it is return to increases again repeating the same behaviours. From these figures, it is noted that the operated range of attack angle increased with increases in the operation wind speed range and then returned to decrease again. The angle of attack range is about (7.73 to 8.23 deg.), (7.91 to 8.64 deg.), and (7.5 to 8.63 deg.) for wind speed of 5m/s, 8m/s, and10 m/s as shown in Fig.14a, Fig.14b, and Fig.14c respectively. Fig.15 illustrates the tangential coefficient of force variation with the attack angle (C_t-α) at different spanwise along of blade length for operating wind speed of 5m/s, 8m/s, and 10m/s respectively. From these figures, generally it is show that, the value of tangential force coefficient was increased until reaching to the maximum value and then decrease gradually until reaching to the minimum values and after this value it is return to increases again repeating the same behaviour. From these figures, it is noticed that the same behaviour appears as shown in Fig.14 but the attack angle range decreases as the turbine blade spanwise station is closer to rotor blade tip. Finally, we can conclude that the hysteresis values of the normal coefficient of force loops is larger than the hysteresis values of the tangential coefficient of force loops.

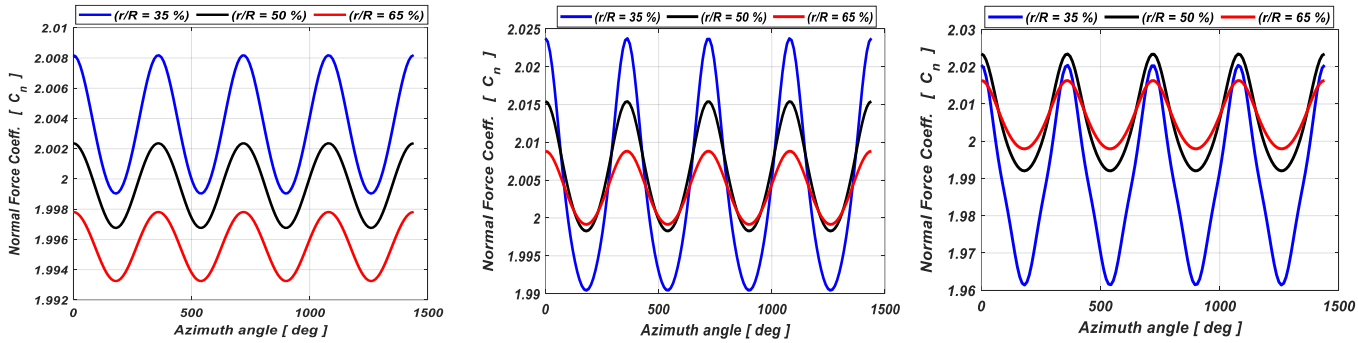

(a) (b) (c)

Fig. 12. Variation of normal coefficient of force with the rotor azimuth angle for several span-wise stations at different operation wind speed and 3 revolutions, (a) At 5m/s, (b) At 8m/s, (c) At 10m/s.

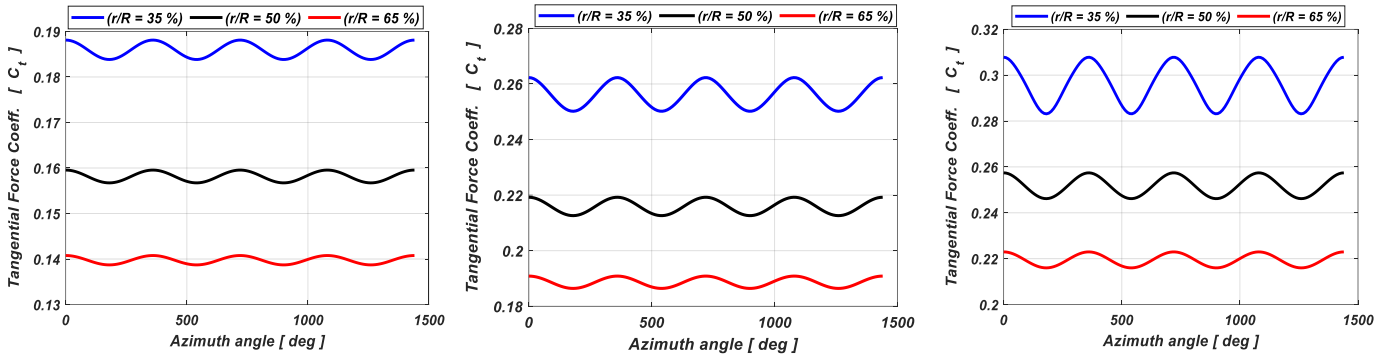

(a) (b) (c)

Fig. 13. Variation of tangential coefficient of force with the rotor azimuth angle for several span-wise stations at different operation wind speed and 3 revolutions, (a) At 5m/s, (b) At 8m/s, (c) At 10m/s.

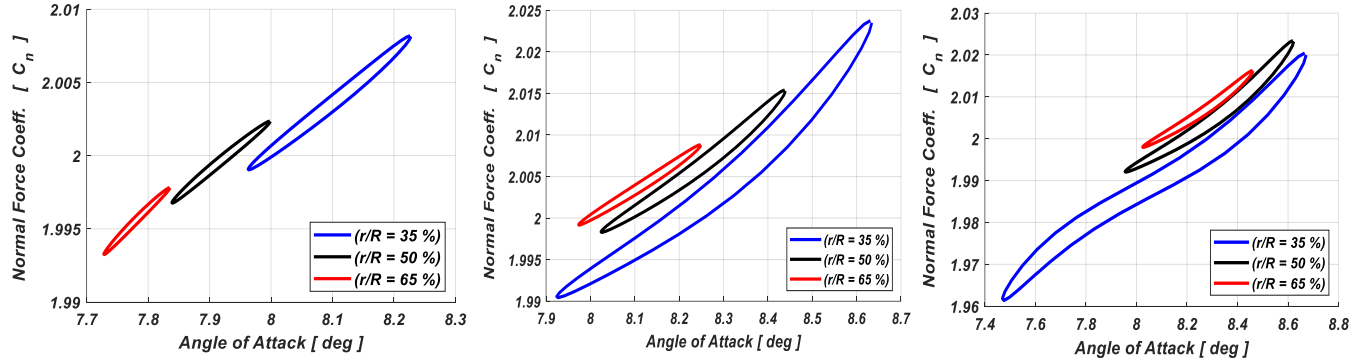

(a) (b) (c)

Fig. 14. Variation of normal coefficient of force with the attack angle for several span-wise sections at different operation wind speed, (a) At 5m/s, (b) At 8m/s, (c) At 10m/s.

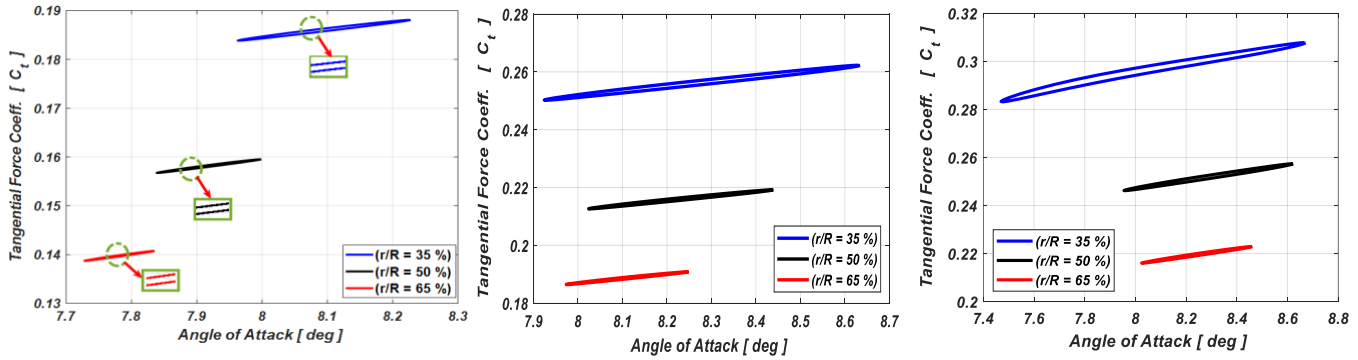

(a) (b) (c)

Fig. 15. Variation of tangential coefficient of force with the attack angle for several span-wise sections at different operation wind speed, (a) At 5m/s, (b) At 8m/s, (c) At 10m/s.

8. Conclusion

In this work, the effects of DS phenomena on the HAWT performance characteristics in the existence of yaw misalignment were study and analysis. The variation of tangential and normal coefficient of force with the turbine rotor azimuth angle and attack angle was predicted at different spanwise along the blade length with emphasis given at Mid-spanwise stations and the loops of C_n-α and C_t-α have been plotted at different stations. The classical DS model of Beddoes–Leishman was used and implemented in conjugated with the BEM generated code to predict the load variation. The advance/retreating blade effect present in this configuration will impose a minimum attack angle (α_{min}) at vertically downward rotor azimuthal position (Ψ=180 degrees) and the maximum incidence (α_{max}) at vertically upward angular coordinate (Ψ=0 degrees). Minding the results obtained, one can come to the following conclusions.

- The up stroke of loop parameters (the time interval when the attack angle is growing) are correspond to the rotor azimuthal positions range from about (180:360 degrees).
- From analogy, the down stroke of loop parameters (the time interval when the attack angle is reducing) are corresponding to the rotor azimuthal positions range from about (0:180 degrees).
- The DS phenomena are occurring mostly at the inboard station along the turbine blade, and then consequentially emphasis was found at the station of about 35% and 50% spanwise. Other radial stations are also addressed during this study.
- After the mid-spanwise stations of the turbine blade the dynamic stall phenomena has low impact.
- After 1-revolution (360 degrees), the obtained results seem to no slower be influenced by the number of revolutions (N). This is mainly because, for all span-wise sections, the variation of normal and tangential force coefficients over the second revolutions (360:720 deg.) is indistinguishable from the curves corresponding to the third revolutions (720:1080 deg).
- The hysteresis values of the normal force coefficient loops are greater than the hysteresis values of the tangential force coefficient loops.
- Finally, we can say that the models of DS have a memory, in the sense that it needs the aerodynamic characteristics of airfoil parameters' history to calculate the instantaneous aerodynamic loads.

According to the above stated conclusions, we can suggest that; using one of the active flow control techniques such as the Co-Flow Jet (CFJ) has more suitable at the inboard stations of the turbine blade and using one of the passive flow control techniques such as the trailing edge flaps (TEF) or tip winglet (TWL) are more effective at the intermediate and outboard stations of the turbine blade. Using these suggested flow control techniques can help to reduce the negative effects of the dynamic stall phenomena on the turbine aerodynamic characteristics, blade fatigue stresses and hence increase the turbine performance characteristics and lifetime of the turbine blades. Finally, according to the energy analysis, the passive and active flow control concept is economical and applicable in controlling the dynamic stall problems.

Declaration of Conflicts of Interests

Funding: Authors state that this research did not receive any specific grant from funding agencies in the public, commercial, or not-for-profit sectors.

Conflicts of interest/Competing interests: Nil

Availability of data and material: Data files are available upon request

References

[1] A. C. Hansen and C. P. Butterfield, "Aerodynamics of horizontal-axis wind turbines." *Annual Review of Fluid Mechanics* 25, no. 1 (1993): 115-149. https://doi.org/10.1146/annurev.fl.25.010193.000555

[2] W. J. McCroskey, " *The phenomenon of dynamic stall* ". No. A-8464. 1981.

[3] L. W. Carr, "Progress in analysis and prediction of dynamic stall." *Journal of aircraft* 25, no. 1 (1988): 6-17. https://doi.org/10.2514/3.45534

[4] D. E. Shipley, M. S. Miller, and M. C. Robinson, M. W. Luttges, D. A. Simms, "*Dynamic stall occurrence on a horizontal axis wind turbine blade*" No. NREL/TP-442-6912; CONF-950116-8. National Renewable Energy Lab. (NREL), Golden, CO (United States), 1995. https://doi.org/10.2172/61151

[5] M. Melius, R. B. Cal, and K. Mulleners. "Dynamic stall of an experimental wind turbine blade." *Physics of Fluids* 28, no. 3 (2016): 034103. https://doi.org/10.1063/1.4942001

[6] E. P. N. Duque, "Navier-Stokes Analysis of Time-Dependent Flows About Wind Turbine." In *Proceedings of the 3rd ASME/JSME joint Fluids Engineering Conference, July18-23, 1999*. 1999.

[7] J. Johansen, N. N. Sørensen, J. A. Michelsen, and S. Schreck. "Detached-eddy simulation of flow around the NREL Phase VI blade." *Wind Energy: An International Journal for Progress and Applications in Wind Power Conversion Technology* 5, no. 2-3 (2002): 185-197. https://doi.org/10.1002/we.63

[8] S. Gupta, and J. G. Leishman. "Dynamic stall modelling of the S809 aerofoil and comparison with experiments." *Wind Energy: An International Journal for Progress and Applications in Wind Power Conversion Technology* 9, no. 6 (2006): 521-547. https://doi.org/10.1002/we.200

[9] X. He-Yong, Q. Chen-Liang, and Y. Zheng-Yin, "Dynamic stall control on the wind turbine airfoil via a co-flow jet." *Energies* 9, no. 6 (2016): 429. https://doi.org/10.3390/en9060429

[10] R. Z. Caglayan, K. Kayisli, N. Zhakiyev, A. Harrouz, and I. Colak, "A Review of Hybrid Renewable Energy Systems and MPPT Methods" International journal of smart grid, Vol.6, No.3, 72–82, September 2022. https://doi.org/10.20508/ijsmartgrid.v6i3.248.g196

[11] R. J. d. A. Vieira, and M. A. Sanz-Bobi, “Power curve modelling of a wind turbine for monitoring its behaviour”, 4th International Conference on Renewable Energy Research and Applications, (ICRERA 2015). https://doi.org/10.1109/ICRERA.2015.7418571

[12] O. ALKUL, D. Syed, and S. Demirbas “A Review of Wind Energy Conversion Systems”, 10th IEEE International Conference on Smart Grid, (icSmartGrid 2022).https://doi.org/10.1109/icSmartGrid55722.2022.9848755

[13] M. B. Farghaly, and E. S. Abdelghany, "Study the effect of trailing edge flap deflection on horizontal axis wind turbine performance using computational investigation." *International Journal of Renewable Energy Research (IJRER)* 12, no. 4 (2022): 1942-1953. https://doi.org/10.20508/ijrer.v12i4.13433.g8617

[14] M. B. Farghaly, A. Aboelezz, "Dynamic Stall Effect on Horizontal Axis Wind Turbine Characteristics for Constant Flow Conditions", Proceedings of ICFD13: Thirteenth International Conference of Fluid Dynamics 21-22 December, 2018, ICFD13-EG-6055.

[15] F. Castellani, D. Astolfi, F. Natili, and F. Mari, "The yawing behavior of horizontal-axis wind turbines: A numerical and experimental analysis." *Machines* 7, no. 1 (2019): 15. https://doi.org/10.3390/machines7010015

[16] F. Samara, and D. A. Johnson, "Experimental load measurement on a yawed wind turbine and comparison to FAST." In *Journal of Physics: Conference Series*, vol. 1618, no. 3, p. 032031. IOP Publishing, 2020. https://doi.org/10.1088/1742-6596/1618/3/032031

[17] W. Wu, X. Liu, J. Liu, S. Zeng, C. Zhou, and X. Wang, "Investigation into yaw motion influence of horizontal-axis wind turbine on wake flow using LBM-LES." *Energies* 14, no. 17 (2021): 5248. https://doi.org/10.3390/en14175248

[18] H. Lee, and D. J. Lee, "Wake impact on aerodynamic characteristics of horizontal axis wind turbine under yawed flow conditions." *Renewable energy* 136 (2019): 383-392. https://doi.org/10.1016/j.renene.2018.12.126

[19] C. Zhu, Y. Feng, X. Shen, Z. Dang, J. Chen, Y. Qiu, Y. Feng, and T. Wang, "Effects of the height and chordwise installation of the vane-type vortex generators on the unsteady aerodynamics of a wind turbine airfoil undergoing dynamic stall." *Energy* 266 (2023): 126418. https://doi.org/10.1016/j.energy.2022.126418

[20] T. Burton, D. Sharpe, N. Jenkins, E. Bossanyi, "Wind energy: handbook”, John Wiley & Sons, Chichester." (2001). https://doi.org/10.1002/0470846062

[21] L. W. Carr, and M. S. Chandrasekhara. "Compressibility effects on dynamic stall." *Progress in Aerospace Sciences* 32, no. 6 (1996): 523-573. https://doi.org/10.1016/0376-0421(95)00009-7

[22] J. G. Leishman, "*Principles of helicopter aerodynamics*" *with CD extra*. Cambridge University Press, 2006.

[23] J. A. Ekaterinaris, G. R. Srinivasan, and W. J. McCroskey, "Present capabilities of predicting two-dimensional dynamic stall." In *AGARD CONFERENCE PROCEEDINGS AGARD CP*, pp. 2-2. AGARD, 1995.

[24] G. R. Srinivasan, J. A. Ekaterinaris, and W. J. McCroskey, "*Dynamic stall of an oscillating wing*", *Part 1: Evaluation of turbulence models*. No. AIAA PAPER 93-3403. 1993.

[25] R. Pereira, G. Schepers, and M. D. Pavel. "Validation of the Beddoes–Leishman dynamic stall model for horizontal axis wind turbines using MEXICO data." *Wind Energy* 16, no. 2 (2013): 207-219. https://doi.org/10.1002/we.541

[26] R. B. d. S. Pereira,. "Validating the Beddoes-Leishman Dynamic Stall Model in the Horizontal Axis Wind Turbine Environment." PhD diss., Master Thesis, Lisbon's Instituto Superior Técnico, 2010.

[27] K. G. Pierce, "Wind turbine load prediction using the Beddoes-Leishman model for unsteady aerodynamics and dynamic stall." Master's thesis, Dept. of Mechanical Engineering, University of Utah, 1996.

[28] J. F. Manwell, J. G. McGowan, and A. L. Rogers, "*Wind energy explained: theory, design and application*. " John Wiley & Sons, 2010. https://doi.org/10.1002/9781119994367

[29] E. Hau, "*Wind turbines: fundamentals, technologies, application, economics*" Springer Science & Business Media, 2013. https://doi.org/10.1007/978-3-642-27151-9

[30] Snel, H., R. Houwink, J. Bosschers, W. J. Piers, G. JW Van Bussel, and A. Bruining. "Sectional prediction of sD effects for stalled flow on rotating blades and comparison with measurements." (1993).

[31] P. K. Chaviaropoulos, and M. O. L. Hansen. "Investigating three-dimensional and rotational effects on wind turbine blades by means of a quasi-3D Navier-Stokes solver." *J. Fluids Eng.* 122, no. 2 (2000): 330-336. https://doi.org/10.1115/1.483261

[32] J. G. Leishman, and T. S. Beddoes. "A Semi-Empirical model for dynamic stall." *Journal of the American Helicopter society* 34, no. 3 (1989): 3-17. https://doi.org/10.4050/JAHS.34.3.3

[33] K. G. Pierce, "Wind turbine load prediction using the Beddoes-Leishman model for unsteady aerodynamics and dynamic stall." Master's thesis, Dept. of Mechanical Engineering, University of Utah, 1996.

[34] J. W. Larsen, S. R. K. Nielsen, and S. Krenk, "Dynamic stall model for wind turbine airfoils." *Journal of Fluids and Structures* 23, no. 7 (2007): 959-982. https://doi.org/10.1016/j.jfluidstructs.2007.02.005